Journal of Engineering and Sustainable Development

Vol.23, No.01 January, 2019
ISSN 2520-0917
https://doi.org/10.31272/jeasd.23.1.8

SLIP DETECTION FOR A SPECIFIC DESIGN OF FINGERTIP IN MULTI-DIRECTION UNDER DIFFERENT LOAD CONDITIONS

Dr. Mauwafak Ali Tawfik [1], Dr. Ihsan Abdulhussein Baqer [2], *Hayder Ahmed Abdulrazzaq[3]

1) Assist Prof., Mechanical Engineering Department, University of Technology, Baghdad, Iraq.
2) Lect., Mechanical Engineering Department, University of Technology, Baghdad, Iraq.
3) Msc.Studenty, Mechanical Engineering Department, University of Technology, Baghdad, Iraq

Abstract: In this paper, a novel design of robotic fingertip has been proposed to detect slippage between the robotic fingertip and the grasped object in multi-direction under different types of loads (static and dynamic loads). The detection process is based on the monitoring of variation in the normal to the tangential component of contact force ratios. The fingertip is composed of a compression springs and a conventional force sensors that are mounted to be able to measure the contact force components continuously. A mathematical model has been derived relative to a proposed design with the help of Matlab-Simulink program. Furthermore, the robotic hand mechanism contains the flexible parts to adapt the grasping force during the slippage occurrence period in spite of the hand actuator is in a stopped status. The grasped object is designed in a cube shape with two unbalance DC motors to generate an excitation that is used as an external dynamic load. The experimental results revealed that the proposed design for detecting slippage in multi-direction is feasible and effective for improving the stability of the grasping process.

Keywords: *Robotic Hand, Fingertip, Grasping, Dynamic Load.*

كشف الانزلاق لتصميم معين لرأس الاصبع في اتجاهات متعددة وتخت ظروف حمل مختلفة

الخلاصة: في هذا البحث، تم اقتراح تصميم جديد لرأس اصبع روبوتي للكشف عن الانزلاق بين مقدمة الاصبع والجسم الممسوك في اتجاهات متعددة وتحت تأثير انواع مختلفة من الاحمال (الحمل السكوني والحمل الجيناميكي). تستند عملية الكشف على رصد الاختلاف في نسبة المركبة العمودية الى المركبة الافقية لقوة التماس. مقدمة الاصبع تحتوي على نوابض انضغاطية وحساسات قوى تقليدية التي تثبت بطريقة لتكون قادرة على قياس مركبات قوة التماس بصورة مستمرة. لقد تم اشتقاق النموذج الرياضي نسبة الى التصميم المقترح ونمذجته بمساعدة برنامج (Matlab-Simulink). علاوة على ذلك فان الية اليد الروبوتية تحتوي على اجزاء مرنة لتكيف قوة الامساك خلال فترى حدوث الانزلاق على الرغم من ان محرك اليد في حالة توقف. كما وقد صمم الجسم الممسوك بشكل متوازي مستطيلات ويحتوي على محركين بتيار مستمر لتوليد استثارة التي تستخدم كحمل ديناميكي خارجي. قد كشفت النتائج العملية بان التصميم المقترح لكشف الانزلاق في اتجاهات متعددة انه قابل للتنفيذ وفعال لتحسين استقرارية عملية الامساك.

1. Introduction and previous work

In general, the tactile sensation represents an important element in the perception of the environment. From human interaction with the undefined environment as well as from physical experience, it is know that slippage preventing plays an essential role in the successful grasping process of an object by robotic or prosthetic hands.

However, especial techniques to detect and prevent slippage have been widely used; almost more studies were focused on applying adequately high and previously known

me.20638@uotechnology.edu.iq

forces to prevent slip [1]. Thus, the main problem is how to save a stable grasp, in spite of it is very difficult to predict the type of the object that will be grasped because there are different types of objects in terms of shape, weight, friction coefficient, stiffness, etc. Furthermore, there are various environmental disturbances (grasped the bottle being hit by means of something else suddenly, water flow into a cup during the grasp period, etc.). Whether the grasping forces are not adequate, the object grasped by the artificial robotic hand will slip. When the slip occurs, the coefficient of friction between the grasped object and the artificial hand decreases to a dynamic status so will be required a greater grasping force to stop the slip [2]. Additionally, if the slippage is not detected at the beginning of occurrence, it may be not stopped at the required time, and may be eventually the grasped object will fall and break down. Consequently, the detection of incipient slip is very significant for artificial hand to re-adjust the grasping force and provide a stable grasp.

Slippage phenomenon can be detected by several methods. Takashi Maeno *et al*. [3] used fifteen strain gauges placed within the finger tips cover and two strain gauges placed into parallel plate on the artificial arm in order to detect slippage by determining the change in stick-slip zones on the elastic finger surface and the change in strain distribution into the elastic finger.

N.I.Glossas *et al*. [4] used an array of tactile sensors called taxels, which consist of 16×16 elements, where the slippage can be detected by changing the position of the maximum concentrated pressure at the finger.

Fusjimoto *et al.* [5] proposed a method to realize the sensation of static friction by using two embedded strips of PVDF films, a different voltage signal will be generated from the two strips of PVDF when the initial slip occurs.

A.Ikeda *et al*. [6] used a force sensor and camera to detect an incipient slip based on estimation of feedback on a visual slip margin where it was estimated by a force sensor to measure the tangential force and a camera to measure the radius of contact region. Yasunori Tada and Koh Hosoda [7] proposed a method to learn a robotic hand the detection of slippage and observed its direction by proposing a sensor network composed of three modalities: piezoelectric film, strain gauge and vision sensor (camera).

Daisuke Gunji *et al.* [8] used the center of pressure (CoP) tactile sensor to detect slippage of a held object where it can determine the position of load distribution center applied to the tactile sensor surface.

Takuya Kawamura et al. [9] proposed a system of hybrid tactile sensors (CMC sensor) for a robotic hand to grasp an object adaptively by measuring slippage of an object, grasping forces, and a silicon rubber deformation of sensor elements. C. Schürmann *et al.* [10] presented a method to detect incipient slippage in high-speed based on resistive sensing principle, which represents a piezoresistive tactile sensor, then using FFT to transform the time series data of tactile sensor to the frequency domain in order to distinguish the type of material.

Pavel Dzitac *et al.* [11] designed and built a functional prototype for manipulation and artificial grasping to detect slippage of the held object and to estimate sufficient grasping forces by using a rotatable roller around the center of its support shaft and a sensor of reflective slippage (CBY70).

Yi zhang *et al*. [12] proposed a method for detecting an incipient slip by using a wavelet transform, the high frequency of the signal of the grasping force was extracted and any sudden change in the wavelet coefficient would be used as an indication for the beginning of the initial slip.

F. Kobayashi *et al*. [13] used force/torque sensor, which measures pressure distribution to detect slip. Rather than increasing gripping force, it was proposed more fingers to be applied in order to stop slipping, from the previous research, the remarks can be concluded as follows: (1) Most literatures focused on the location of the sensor so as not to affect the performance of the robotic or prosthetic hands; (2) Some approaches have been used a camera as a vision sensor to estimate the eccentricity degree of contact region, with this approach there is a problem, how to embed camera in relatively small size places like hands. Moreover, processing speed based on the number of frames per second (frame rate) of vision, and achievement detection slippage at high speeds is generally difficult; (3) Some of researchers weren't invented novel sensing technologies, but incorporated different kinds of sensors; (4) Detection slippage by estimation the coefficient of friction, this technique is not accurate and indirect measurement. Additionally, it is not working in undefined environment; (5) Detection slippage by determining the changes in the foot-print of contact over tactile sensors: the changes in shape of grasping area and the changes in the distribution of the pressure-force, this technique is not affected when the held object is flexible and when slipping is the result of the dynamic load effect.

In the present paper, the working principle of our approach based on sensing whole contact force components, i.e. the normal and two tangential components after that the two tangential to normal force ratios will be computed which remain constant during the case of stable grasp and will change when the object begin to slip [14]. To embrace this approach, a new design of the fingertip is proposed for detecting slippage of the grasped object under different load conditions. The proposed design deals with conventional sensors that have the ability to measure only the applied forces in the normal direction, but in the present work, they employed to measure forces in three dimensions by processed the signals through a mathematical model. Also, the advantage of the proposed system can detect the slip without knowing any characteristic of the grasped object such as weight, coefficient of friction, shape, surface texture and the type of the excitation exerted upon the grasped object.

2. The Dynamic Modeling

Fig.1shown below represents a fingertip mechanism of artificial hand, which is designed as a dome-shape that represents the area of contact that occurs with the grasped object, also it's connected with the links that make up the finger by the ball joint**.**

The fingertips were covered with a viscoelastic material, which have a ridged surface, in order to produce a small vibration at the moment of slip occurrence as well as provide more reliable properties of friction than smooth skin [15].

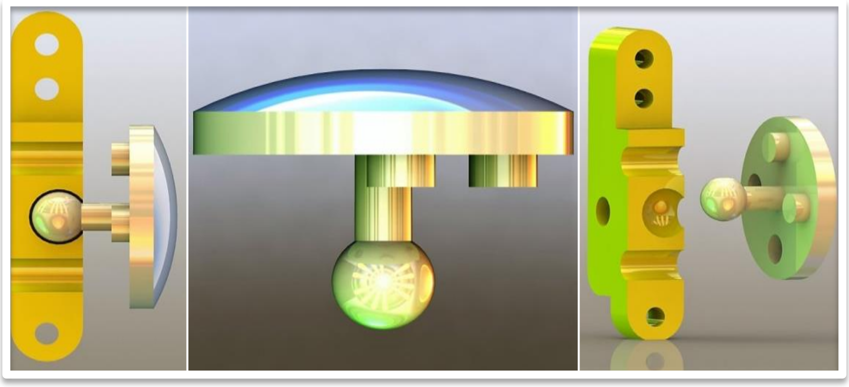

(A) (B) (C)

Figure 1. The proposed Mechanism of the artificial fingertip

- (A) Side view of fingertip part and its frame
- (B) Side view of Fingertip part
- (C) 3D view, fingertip part release from its frame

The mathematical model of the artificial fingertips has been derived to create the relationship between the components of the contact force and the forces exerted on force sensor .The desgin of fingertip by using solid work program has been shown in fig .2.

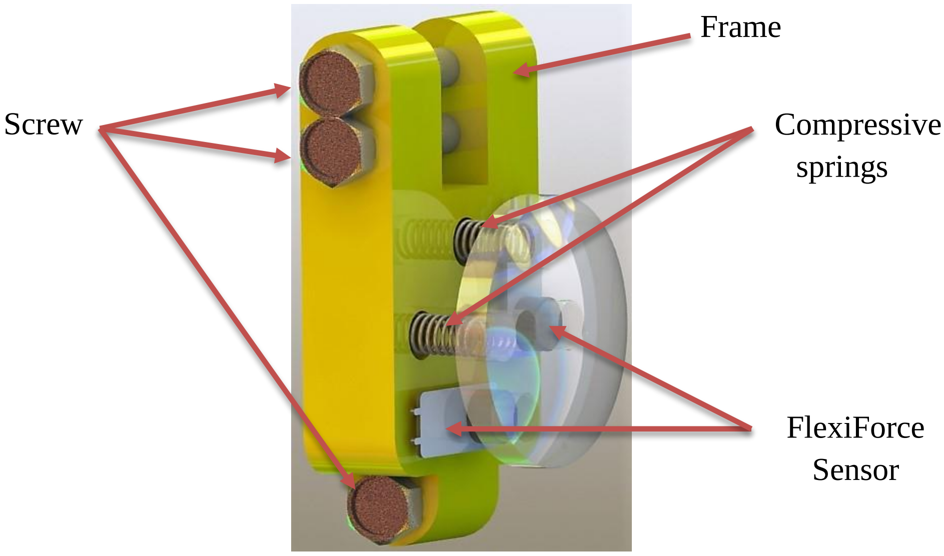

Figure 2. FlexiForce Sensors and Springs Mounting with Fingertip

For simplification, it can be assumed that there is no relative motion between the fingertip and the grasped object before slip occurrence; also, the ball joint friction and the inertia of the fingertip have been neglected [16]. Fig.2. represents the distribution of contact force components, forces exerted on sensors and springs forces where these forces can be analyzed statically to find both normal and tangential force component with respect to force sensors.

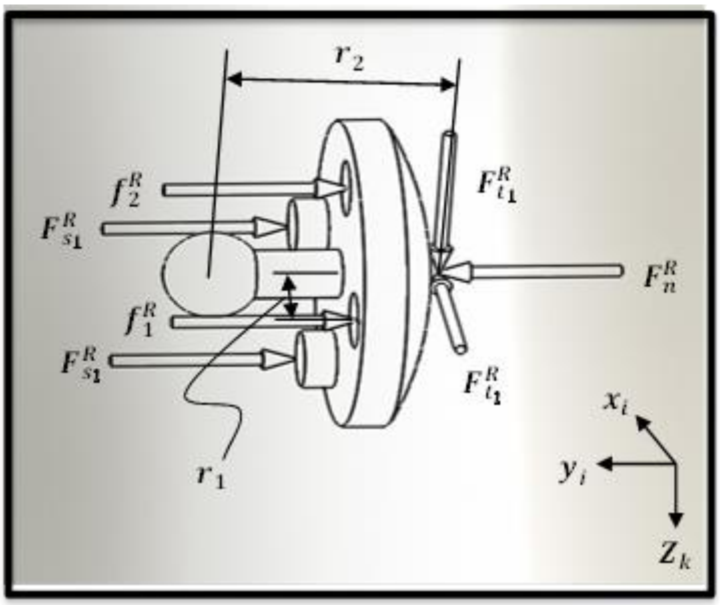

Figure 3. Fingertip Free Body Diagram.

By taking summation of forces in y-axis the normal force can be found:

$$F_n^R = F_{s_1}^R + F_{s_2}^R + f_1^R + f_2^R \tag{1}$$

From the moment equilibrium equations of the fingertip in three axes as a vector about its ball joint the two tangential forces can be determined as follows:

$$\left(F_{t_1}^R i * r_2 j\right) + \left(F_{t_2}^R k * r_2 j\right) + (f_1^R j - r_1 i) + (f_2^R j - r_1 k) + \left(F_{s_1}^R j * r_1 i\right) + \left(F_{s_2}^R j * r_1 k\right) = 0$$

For $i = i$ & $k = k$, and after mathematical simplification, the following will be true:

$$F_{t_1}^R = \frac{f_1^R * r_1 \;+\; F_{s_1}^R * r_1}{r_2} \tag{2}$$

And,

$$F_{t_2}^R = \frac{f_2^R * r_1 \;+\; F_{s_2}^R * r_1}{r_2} \tag{3}$$

By the same way, the normal and tangential force components of the left finger will be:

$$F_n^L = F_{s_1}^L + F_{s_2}^L + f_1^L + f_2^L \tag{4}$$

$$F_{t_1}^L = \frac{f_1^L * r_1 \;+\; F_{s_1}^L * r_1}{r_2} \tag{5}$$

And,

$$F_{t_2}^L = \frac{f_2^L * r_1 \;+\; F_{s_2}^L * r_1}{r_2} \tag{6}$$

Now, dividing the two tangential forces of each finger on their normal forces in order to obtain ratios of contact force components in Z-axis and X-axis as follows:
In Z-axis:

$$F_{t_1}^R / F_n^R = \frac{f_1^R * r_1 + F_{s_1}^R * r_1}{(F_{s_1}^R + F_{s_2}^R + f_1^R + f_2^R) * r_2} \quad , \quad F_{t_1}^L / F_n^L = \frac{f_1^L * r_1 + F_{s_1}^L * r_1}{(F_{s_1}^L + F_{s_2}^L + f_1^L + f_2^L) * r_2} \tag{7}$$

And in X-axis:

$$F_{t_2}^R / F_n^R = \frac{f_2^R * r_1 + F_{s_2}^R * r_1}{(F_{s_1}^R + F_{s_2}^R + f_1^R + f_2^R) * r_2} \quad , \quad F_{t_2}^L / F_n^L = \frac{f_2^L * r_1 + F_{s_2}^L * r_1}{(F_{s_1}^L + F_{s_2}^L + f_1^L + f_2^L) * r_2} \tag{8}$$

From the stable grasp status and the coefficient of friction cone definition, the contact force component ratio must be within the friction cone,

$$\frac{F_{t_i}}{F_{n_i}} \leq \mu_i \tag{9}$$

But whether the texture of the surface of the grasped object is unknown, i.e. the coefficient of friction is unknown. In this case, the slippage cannot be distinguished by using equation (9). So, the slip detection should be done through monitoring the variation in the result of an equation (8) with the real time.

3. System Description

Robotic gripper: an artificial two-finger gripper was set up at the end of 4degreese of freedom artificial robotic arm. The robotic gripper is underactuated as shown in figure (4), where it consists of DC geared motor which is connected to power screw in order to convert the motion from rotational at the DC motor to linear at constrained nut, then the nut connect with three springs that transmit the linear motion to cylindrical part which associated with the links which form the fingers structure. Connection the springs between the nut and the cylindrical part allows the artificial hand to adapt the grasping force in spite of the actuator is in a stationary status.

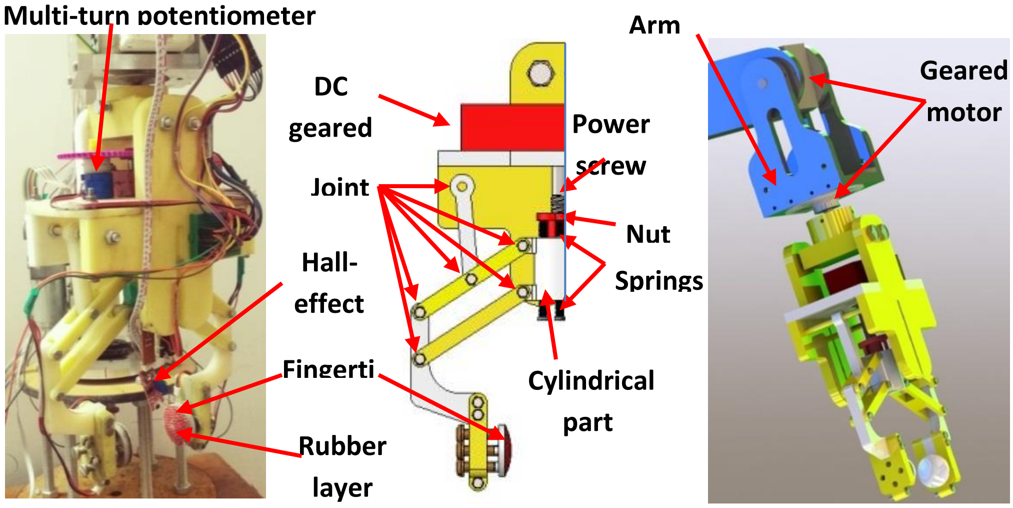

Figure 4. Robotic gripper mechanism

Sensors: A FlexiForce sensor model A301 [17] has been used in this work, where it mounted within the fingertip. It can measure the applied force on its sensing area in one direction, but in this work it is used to measure contact force components in three dimensions with 445 N range of force. Also, a hall-effect sensor 49E model [18] has been used to give an indication of the situation of slippage by observing the variation in relative motion between the palm of gripper and the grasped object, as clarified in fig.4.

The signal of the hall-effect device was not calibrated because it is used only for slip monitoring. All the mentioned sensors generate an analog signal that are transformed to digital signal from a data acquisition device (National Instruments USB-6009), and then the digital signal is transmitted to a PC in order to process it by Matlab-Simulink program.

Grasped Object: The grasped object is designed in a cuboid shape with two disturbance generators (unbalance DC motors) embedded within the grasped object as clarified in fig.5 to generate an excitation that used as external dynamic load. Each two corresponding layer at the contact zone of the grasped object with the fingertip is covered by one type of selected material, namely, glass and wood layers as the test requires as shown in fig. 5a and 5b.

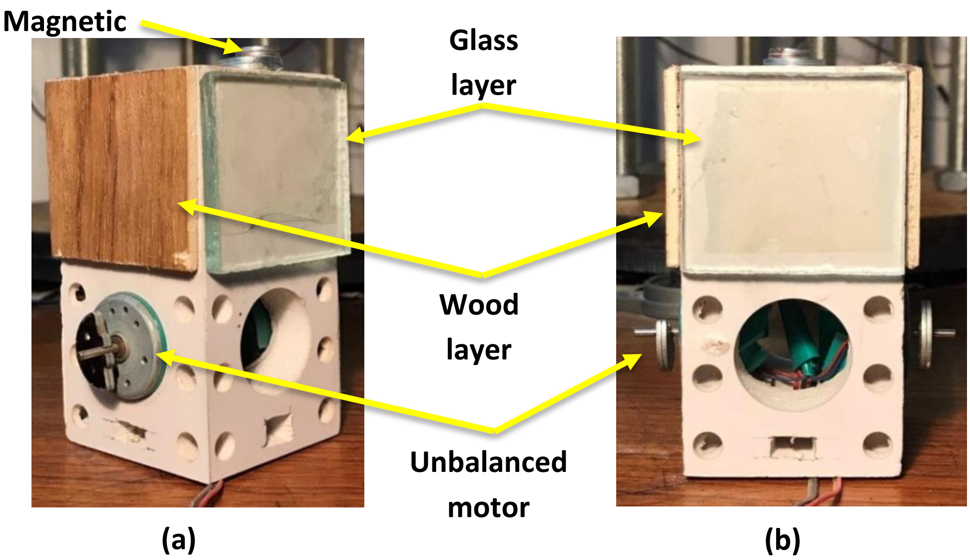

Figure 5. (a) 3D view and (b) side view of experimental object

4. Slipping Experiments and Discussion

The objective of these experiments is to demonstrate the effectiveness of the proposed system to detect slipping in multi-direction under different types of loads. The experiments will be explained as follows:

4.1 First Experiments Group

grasping the object without external disturbances.

This group of experiments is performed based on the following sequence:

(1) Grasping the object by means of turning-on manually the robotic gripper actuator until it reaches the stable status of grasp;

(2) Start recording the signals of the sensory system at the moment when the grasping reaches the stable status;

(3) Pulling the grasped object manually until it starts to slip;

(4) Restarting the previous steps but in different slippage direction and pair of contact material (wood, glass)

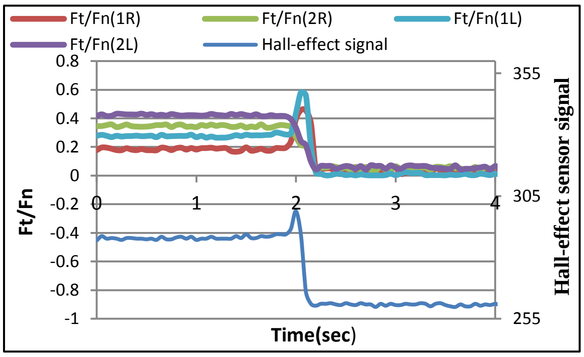

Figure 6. The force ratio with angle slipping 0, glass layer

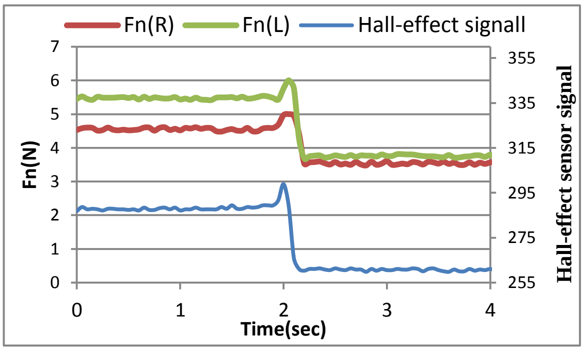

Figure 7. The normal force component with angle slipping 0, glass layer

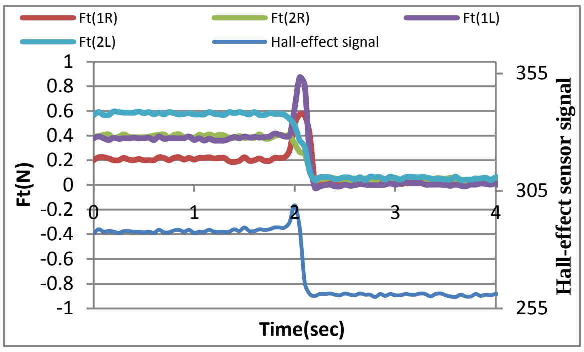

Figure 8. The tangential force component with angle slipping 0, glass layer

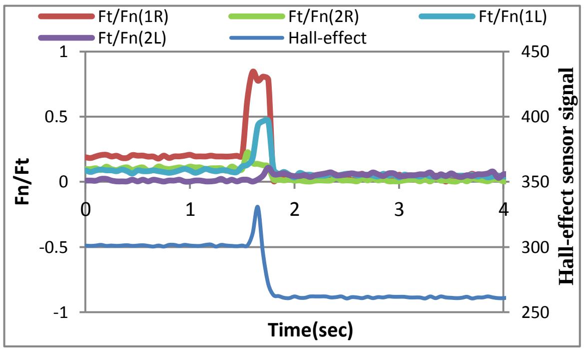

Figure 9. The force ratio with angle slipping 0, wood layer

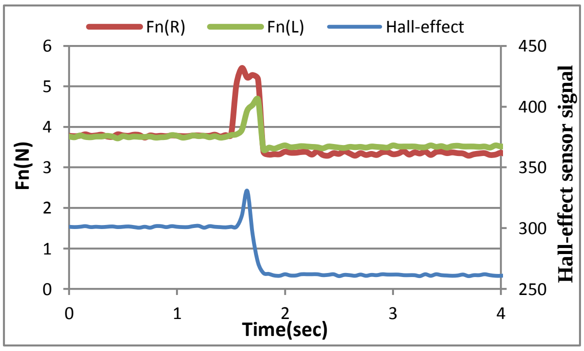

Figure 10. The normal force component with angle slipping 0, wood layer

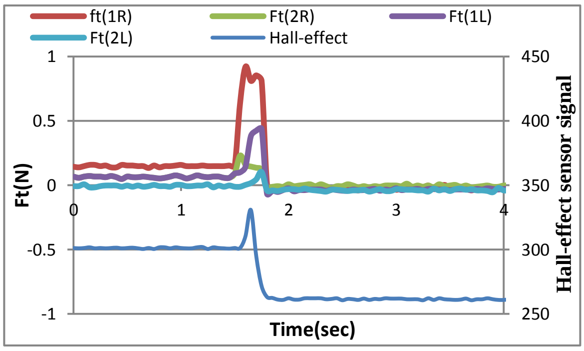

Figure 11. The tangential force component with angle slipping 0, wood layer

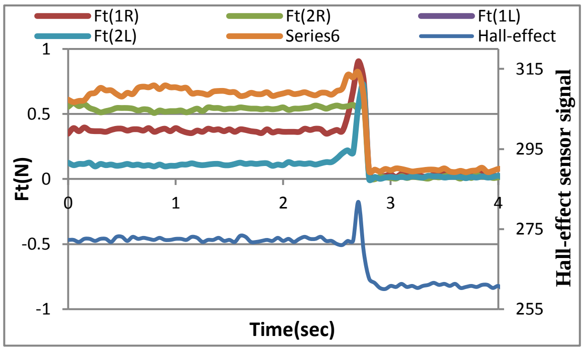

Figure 14. The tangential force component with angle slipping 40, glass layer

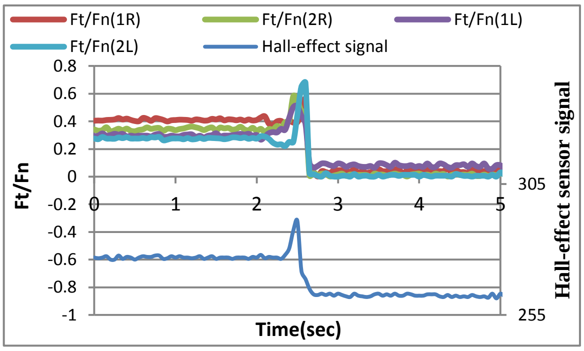

Figure 15. The force ratio with angle slipping 40, wood layer

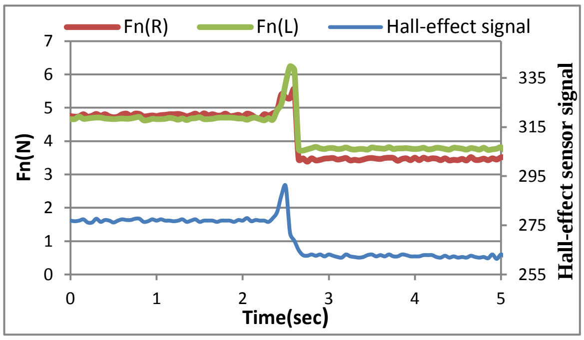

Figure 16. The normal force component with angle slipping 40, wood layer

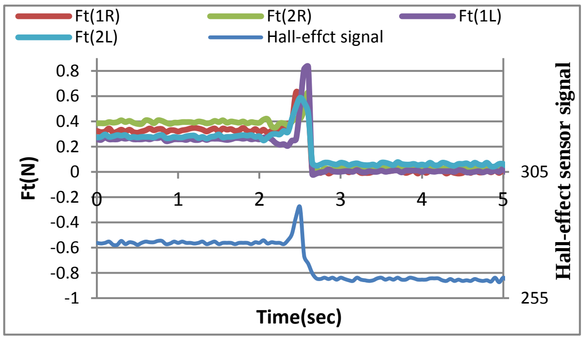

Figure 17. The tangential force component with angle slipping 40, wood layer

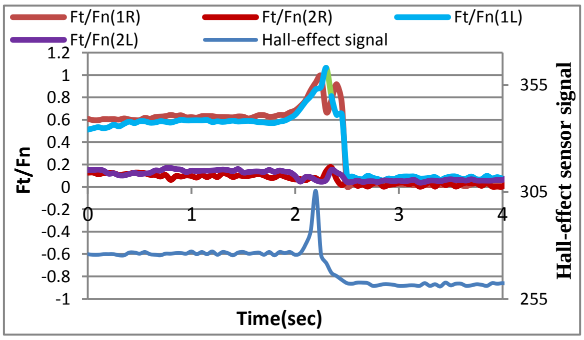

Figure 18. The force ratio with angle slipping 90, glass layer

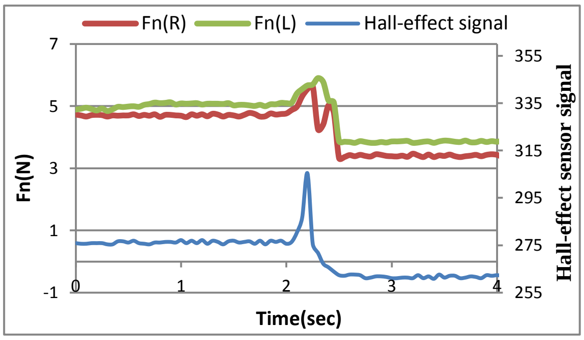

Figure 19. The normal force component with angle slipping 90, glass layer

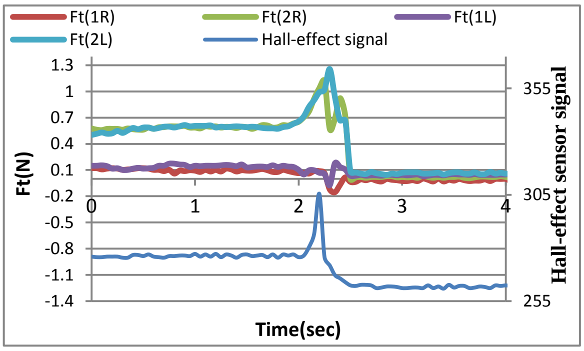

Figure 20. The tangential force component with angle slipping 90, glass layer

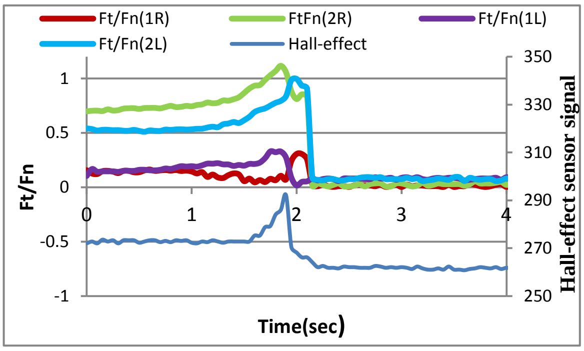

Figure 21. The force ratio with angle slipping 90, wood layer

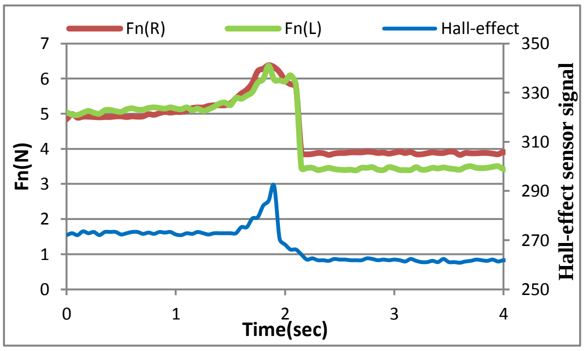

Figure 22. The normal force component with angle slipping 90, wood layer

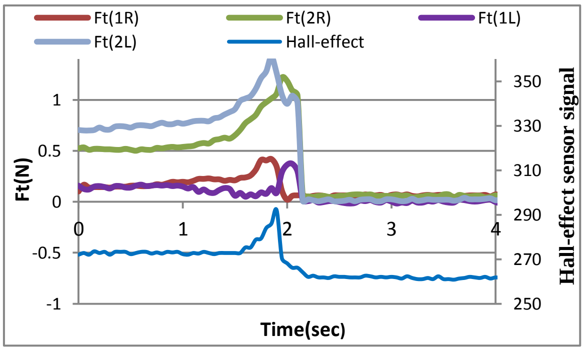

Figure 23. The tangential force component with angle slipping 90, wood layer

From the results of first experiments group, one can observe that the signal behavior of contact force components ratio in real time start with a certain ratio of initial grasping force components. This force ratio varies from one to another experiment due to the effect of flexible parts (compressive springs) in the fingertip structure, then this signal will vary as a jump from the initial value at the moment of slip occurrence. Also at this time, the variation in the Hall-effect sensor signal will be occurred approximately similar to the variation in the signal of force ratio, this means the beginning of the grasped object slippage. Furthermore, it was observed that the variation in the signal of ratios (F_{t_i}/F_{n_i}) changes according to the angle of slippage occurrence. When the slippage angle is 0, the jump in signal just occurs in the force ratios that are oriented towards z-axis, when the slippage angle is 40, the jump in the signal occurs at all the force ratios in x-axis and z-axis in a similar behavior, and when the slippage angle is 90, the jump in signal just occurs in the force ratios that are oriented towards the x-axis.

4.2 Second Experiments Group

grasping the object under disturbance (dynamic load).

These experiments are performed based on the pervious sequence as mentioned in the first group of experiments except step 3, However in these experiments the unbalance motors have been used as disturbance generators in order to generate slippage between the grasped object and the fingertip at the moment of it's turning-on. The results of this group will be listed and presented in fig. 24 to 41:

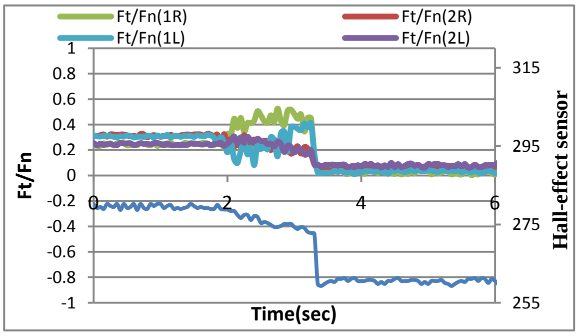

Figure 24. The force ratio with angle slipping 0, glass layer

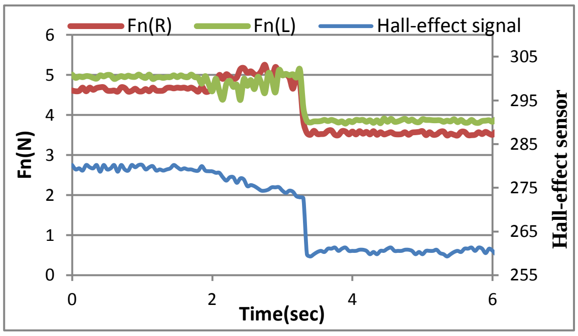

Figure 25. The normal force component with angle slipping 0, glass layer

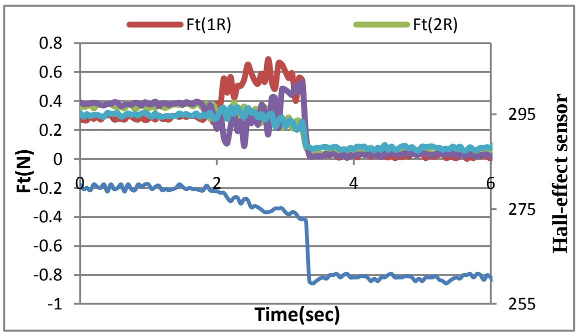

Figure 26. The tangential force component with angle slipping 40, glass layer

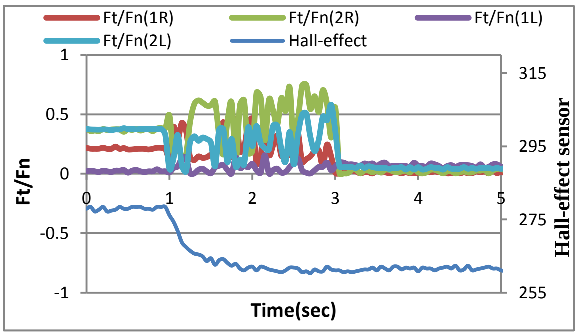

Figure 27. The force ratio with angle slipping 0, wood layer

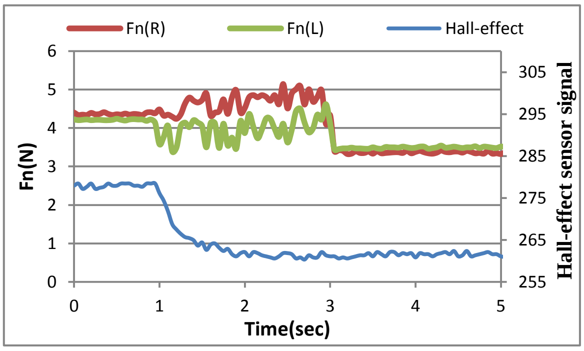

Figure 28. The normal force component with angle slipping 0, wood layer

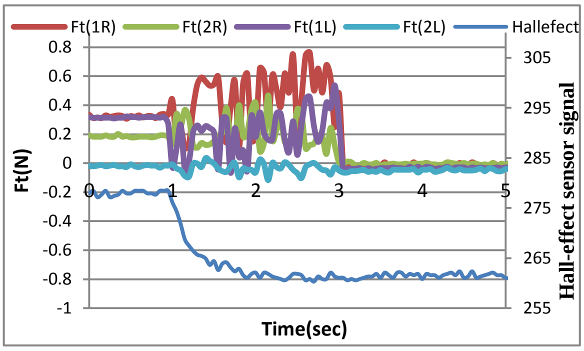

Figure 29. The tangential force component with angle slipping 40, wood layer

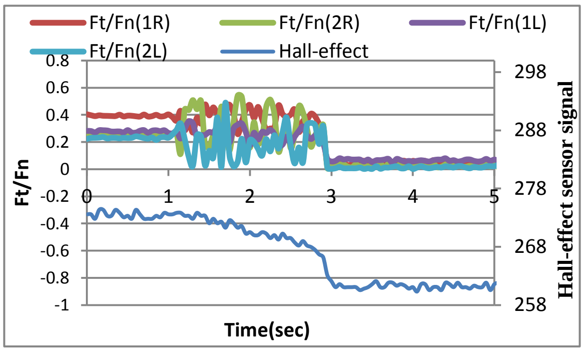

Figure 30. The force ratio with angle slipping 40, glass layer

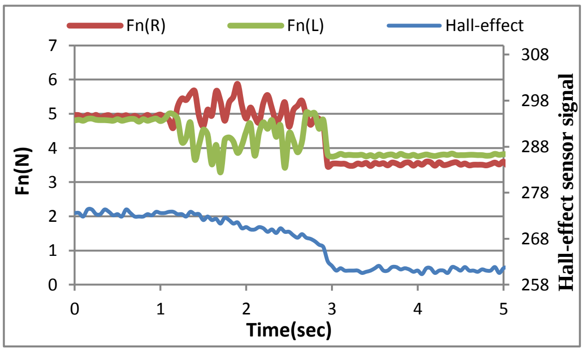

Figure 31. The normal force component with angle slipping 40, glass layer

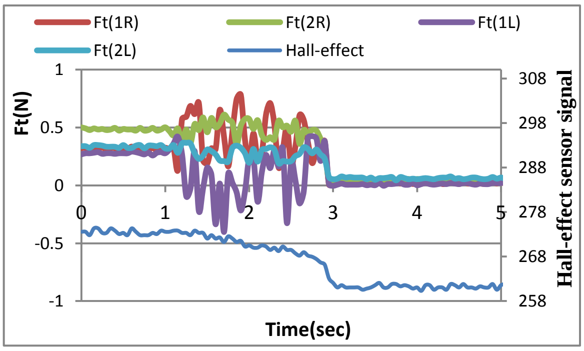

Figure 32. The tangential force component with angle slipping 40, glass layer

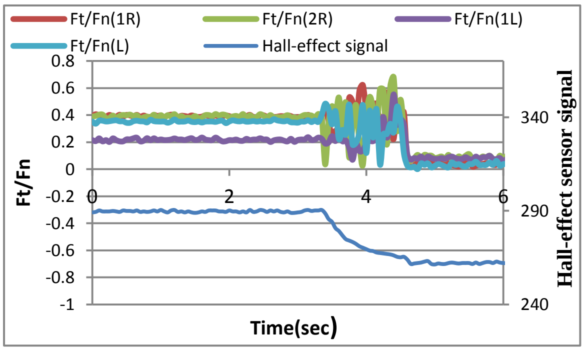

Figure 33. The force ratio with angle slipping 40, wood layer

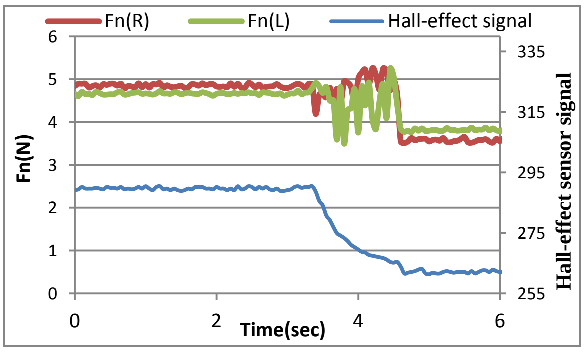

Figure 34. The normal force component with angle slipping 40, wood layer

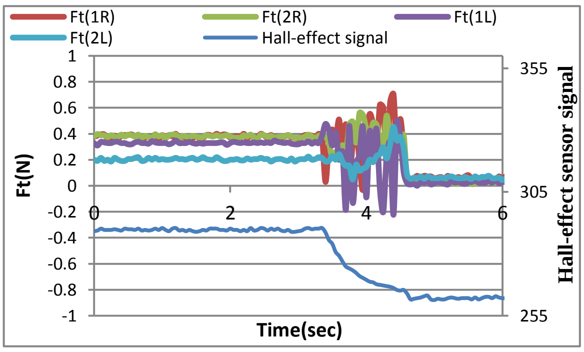

Figure 35. The tangential force component with angle slipping 40, wood layer

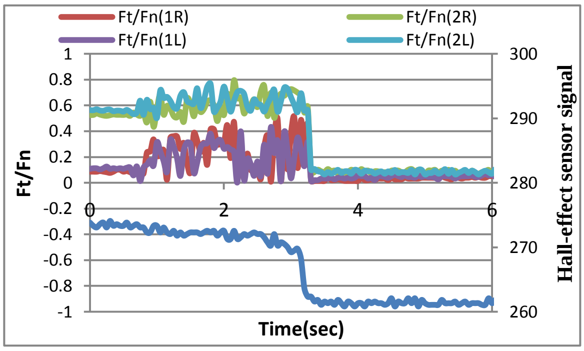

Figure 36. The force ratio with angle slipping 90, glass layer

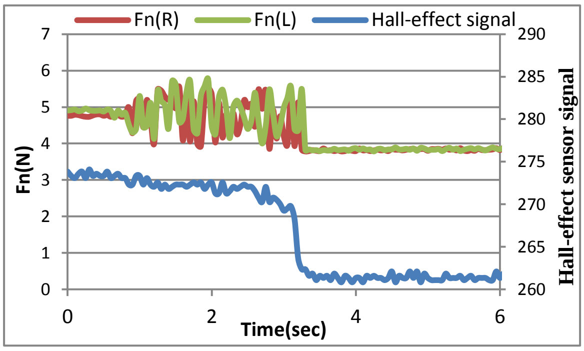

Figure 37. The normal force component with angle slipping 90, glass layer

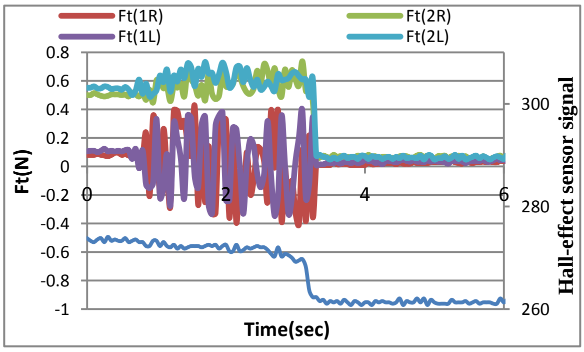

Figure 38. The tangential force component with angle slipping 90, glass layer

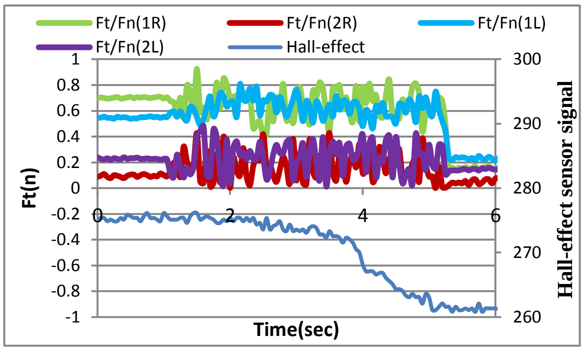

Figure 39. The force ratio with angle slipping 90, wood layer

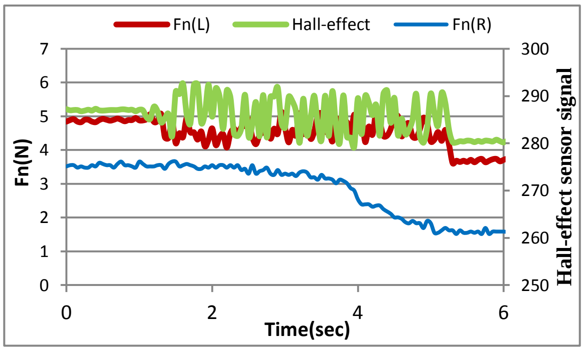

Figure 40. The normal force component with angle slipping 90, glass layer

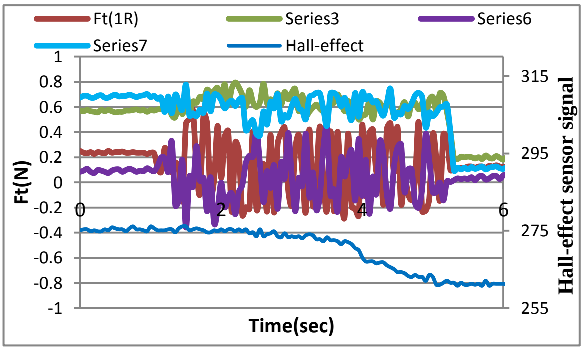

Figure 41. The tangential force component with angle slipping 90, glass layer

In these experiments, when the dynamic load is applied, the object begins to slip, also at this moment; the signal of force ratio is starting to change in a form of an alternative sequence, this change is due to the instantaneous variation that occurs in the magnitude and direction of the contact force components. Subsequently, the friction cone condition cannot be satisfied because of the variation range of force ratio it will be raised at the period of slippage occurrence in comparison with the drop in friction coefficient from static state (μ_s) to dynamic state (μ_d). Also, it was observed that the response of the contact force components ratios varies depending on the angle of slip, namely, only the ratio that is towards the angle of slip will get the variation in its signal as explained in the first group of experiments.

From results of all experiments, one can deduce that the components of contact force which have the same direction of the slip also have the same behavior, so any force ratio (F_{t_i}/F_{n_i}) shows this behavior firstly can be considered to distinguish the onset of slippage. This increase in the force ratio signal can be interpreted as a result of applying an external load whether it is quasi-static load or dynamic load on the grasped object, this leads to an increase in the magnitude of the normal component and the two tangential components of contact force but in different rates. Additionally, it was observed, when the contacting occurs between the rubber layers of fingertips and the pair of glass layers of grasped object, the grasping process is more stable and the results of experiments of this case shows best responses to the slippage occurrence, since the mechanism of adhesion friction is into play [19]. But when the contacting occurs between the fingertips rubber layers and the pair of wood layers of the grasped object, the experimental results of this case of contact shows different responses, because they were confusingly and noisy, this is due to the variety in mechanism of friction of rubber with wood. As summarized, the present approach can detect the onset of slip of the grasped object with different roughness i.e. smooth layer (glass) and rough layer (wood).

5. Conclusions

A novel design of robotic fingertip has been designed to be able to detect slippage in multi-directions under different type of load (static load and dynamic load) with different contacting layers (glass on rubber and wood on rubber) by measuring the components of contact force in three dimensions by implementing conventional sensor. An underactuated artificial gripper was designed with linkages mechanism. A grasped object was designed in a cubic shape with two unbalance DC motors embedded within the grasped object structure. The generated signal for slippage detection demonstrates a feasible behavior that can be aid to improve the stability of the grasping process.

6. References

1. Becedas, J. Payo, I. Feliu, V. (2011)."*Two-flexible-fingers gripper force feedback control system for its application as endeffector on a 6 dof manipulator*". IEEE Transactions on Robotics, Vol. 27, pp. 599-615.
2. Y. Itp, Y. Kim, and G, obinata**,** (2011).**"***Robust slippage degree estimation based on reference update of vision-based tactile sensor*", IEEE Sensors J., vol. 11, no. 9, pp. 2037-2047.
3. Takashi Maeno, Shinichi Hiromitsu and Takashi Kawai, (2000). "*Control of Grasping force by Detecting Stick/Slip Distribution at the Curved Surface of an Elastic Finger*", In Proceedings of IEEE International Conference on Robotics and Automation, Vol.4, pp.3896-3901.
4. N. I. Glossas and N. A. Aspragathos, (2001). "*Fuzzy Logic Grasp Control Using Tactile Sensors*", Mechatronics, Vol.11, Issue.7, pp.899-920.
5. I. Fusjimoto, Y. Yamada, T. Maeno, (2003). "*Development of Artificial Finger Skin to Detect Incipient Slip for Realization of Static Friction Sensation*", In Proceedings of IEEE International Conference on Multisensor Fusion and Integration for Intelligent Systems MFI, pp.15-21.
6. A.Ikeda, Y.Kurita, J.Ueda, Y.Matsumoto, T.Ogasawara, (2004). "*Grip Force Control for an Elastic Finger using Vision-based Incipient Slip Feedback*", In

Proceedings of IEEE International Conference on Intelligent Robots and Systems, Sendai, Japan.

7. Yasunori Tada and Koh Hosoda, (2006). "*Acquisition of Multi-Modal Expression of Slip through Pick-Up Experiences*", In Proceedings of IEEE/RSJ International Conference on Intelligent Robots and Systems, Beijing, China.
8. Daisuke Gunji, Yoshitomo Mizoguchi, Seiichi Teshigawara, Aiguo Ming, Akio Namiki, Masatoshi Ishikawaand and Makoto Shimojo, (2008). "*Grasping force control of multi-fingered robot hand based on slip detection using tactile sensor*", In Proceedings of IEEE International Conference on Robotics and Automation, CA, USA.
9. Takuya Kawamura, Naoto Inaguma, Ko Nejigane, Kazuo Tani and Hironao Yamada, (2012). "*Measurement of Slip, Force and Deformation Using Hybrid Tactile Sensor System for Robot Hand Gripping an Object*", International Journal of Advanced Robotic Systems, Japan.
10. C. Schürmann, M. Schöpfer and R. Haschke, (2012). "*A High-Speed Tactile Sensor for Slip Detection", Springer Tracts in Advanced Robotics*, pp 403-415.
11. Pavel Dzitac, Abdul Md Mazid, M. Yousef Ibrahim, Gayan Kahandawa Appuhamillage and T. A. Choudhury, (2015). "*Friction-based slip detection in robotic grasping*", Industrial Electronics Society, IECON 2015 - 41st Annual Conference of the IEEE, Yokohama, Japan.
12. Yi Zhang, Xiao-Gang Duan, Guoliang Zhong and Hua Deng, (2016). "*Initial Slip Detection and Its Application in Biomimetic Robotic Hands*", IEEE Sensors Journal , Vol. 16, Issue. 19.
13. F. Kobayashi, H. Kanno, H. Nakamoto, and F. Kojima**,** (2014). "*Slip based pick-and-place by universal robot hand with force/torque sensors*", in IEEE Symposium on Robotic Intelligence in Informationally Structured Space, pp.1-4.
14. Nacy, S. M., Tawfik, M. A., Baqer, I. A. (2014)."*A novel fingertip design for slip detection under dynamic load conditions*", ASME Journal of Mechanisms and Robotics, Vol.6/ 031009-1.
15. Marc R. Tremblay and Mark R. Cutkosky, (1993). "*Estimating Friction Using Incipient Slip Sensing during a Manipulation Task*", Proceeding of IEEE International Conference on Robotics and Automation, Vol.1, pp.429-434, Atlanta-Georgia-USA.
16. Fanny Ficuciello, (2010). "*Modeling and Control for Soft Finger Manipulation and Human-Robot Interaction*", Ph.D Thesis, Faculty of Engineering, University of Naples FedricoII, page (23).
17. "*FlexiForce® Standard Model A301*" online available (https://www.tekscan.com/products-solutions/force-sensors/a301).
18. "*Hall-Effect Sensor 49E*", online available (https://chioszrobots.com/2015/03/26/hall-magnetic-standard-linear-module-arduino-projects-robots-new/).
19. B. N. J. Persson, (2001). "*Theory of Rubber Friction and Contact Mechanics*", Journal of Chemical Physics, Vol.115, No.8, pp.3840-3861.